Hindawi
Advances in Civil Engineering
Volume 2023, Article ID 6672667, 11 pages
https://doi.org/10.1155/2023/6672667

Research Article

Borehole TV Imaging Technology for Horizontal Directional Drilling Based on an Optimization Algorithm for Structural Planes

Dong Yang[1], **Wangsuo Cai**[2], **Junchao Wang**[1] and **Yong Fang**[1]

[1]*Chengdu Huajian Geological Engineering Technology Co., Ltd, Chengdu 611734, China*
[2]*Sichuan Water Development Investigation, Design & Research Co., Ltd., Chengdu 610097, China*

Correspondence should be addressed to Dong Yang; 271062514@qq.com

Received 6 July 2023; Revised 23 August 2023; Accepted 25 August 2023; Published 18 October 2023

Academic Editor: Qingchao Li

The horizontal directional drilling technology combined with the borehole TV imaging technology can be used to obtain most of the geological information in conventional adit exploration. This combination has little impact on the environment and is free from topographic constraints, thus contributing to green exploration. However, conventional algorithms for structural planes fail to accurately extract information on the attitudes of incomplete structural planes in boreholes of any azimuth. Moreover, existing borehole TV devices are mostly cable-based and, thus, difficult to put in place in horizontal drilling. They are prone to get stuck in the collapse section of boreholes, thus damaging the devices. Given these challenges, this study develops an optimization algorithm for structural planes: (1) first, information on multiple points in the 2D unfolded view is fitted using a sinusoidal function curve, three arbitrary points are constructed using the fitted curve, and the normal vector of the plane determined by the three points is calculated; (2) the normal vector in the geodetic coordinate system is obtained after two rotations of the spatial coordinate system based on the theory of transformation of Cartesian coordinate system; (3) finally, the dip angle and dip direction of a structural plane are calculated using the normal vector in the geodetic coordinate system. By making the best use of the information on multiple points in the 2D unfolded view, the optimization algorithm can overcome the defect that is difficult for conventional two-point methods to locate the highest and lowest points of discontinuous structural planes. Therefore, the optimization algorithm applies to calculating the attitudes of structural planes in boreholes of any azimuth. Based on this optimization algorithm, this study successfully develops a cable-free, storage-based TV device for boreholes of any azimuth. This device was employed for laboratory experiments on 20 complete structural planes and 32 incomplete structural planes. As indicated by the experiment results, the optimization algorithm proposed in this study is applicable to many types of structural planes, with a dip direction error of less than 10° and a dip angle error of less than 5°, thus meeting the production requirements.

1. Introduction

To ascertain the properties of deep strata and use adits for in situ testing, it is always necessary to deploy adit explorations at the tunnel inlets and outlets of major engineering and in areas subjected to major geological problems. However, adit construction suffers serious safety hazards and low efficiency (tunneling for 3–4 m/day) and is environmentally unfriendly. For tunnels with a burial depth of more than 1,000 m, vertical drilling is often difficult or impossible due to topographic and traffic conditions. In recent years, horizontal directional drilling has rapidly developed. This technology is characterized by high construction efficiency (daily drilling depth: about 15–30 m) and low environmental impact. In addition, it is free from topographic influence, thus the drilling construction can be arranged directly along the tunnel axis [1–3]. This technology, combined with integrated logs and the images and videos of the cores and panoramic views of boreholes, allows for acquiring most of the geological information required for conventional adit explorations, precisely investigating the lithological changes of surrounding rocks, the density of joint fissures, and the distribution of fault fracture zone, and accurately classifying tunnels' surrounding rocks [4–6].

Borehole TV devices have developed for decades from the early literally rotating and front-view panoramic borehole TV devices into the widely used panoramic borehole camera systems [7, 8]. With the progress in camera technology in recent years, some higher-definition and more intelligent borehole TV devices have been developed [9–11]. Some specific interpretation software has also been developed, such as the AutoLISP program for the construction of geological cross-sections [12] and the Borehole and Ice Feature Annotation Tool [13]. The borehole TV imaging technology has been widely applied to in situ measurements in the fields of tunnel surveying [4–6], hydropower engineering [14], hydrological exploration [15–17], hydrocarbon storage [18–21], and sedimentary structures [22]. The borehole TV imaging technology, which is independent of the core drilling process, can directly obtain the borehole rock images and the occurrence of the in situ structural planes on the borehole wall. It allows for more types of in situ tests if combined with other sensors or devices [23, 24].

Despite numerous advantages, the borehole TV imaging technology still faces two major burning challenges when applied to horizontal directional drilling. One challenge is that present TV devices are mostly cable-based devices [9–11], which enable logging while descending under the action of dead weight in vertical boreholes but can only be pushed forward using a drill rod in horizontal boreholes. The presence of signal cables makes it difficult to push forward the TV devices, which are prone to be stuck in the fractured sections of boreholes. Moreover, signal cables are easily worn, and the devices are prone to be damaged, causing logging failure.

The other challenge is a lack of precise analysis of the attitudes of structural planes obtained based on the panoramic imaging of horizontal directional drilling. Presently, the automatic identification of structural plane characteristics based on the image processing technology has been widely applied and developed [25–28]. The intersections between the structural planes in a borehole and the borehole wall are present as approximate ellipses in the 3D space and as sinusoidal curves in 2D images [29–31]. For the images of vertical boreholes, the sinusoidal functions of the intersected structural planes can be determined using the coordinates of the highest and lowest points on the sinusoidal curves, and then the dip angles and directions of structural planes can be calculated [31]. However, in some cases, it is difficult to locate the highest and lowest points of a discontinuous structural plane, making this two-point-based method unworkable. Moreover, the analytical solution is the attitude of a structural plane under local coordinates of the working face and, thus, cannot be directly used for horizontal or inclined boreholes. A method for calculating the attitudes of structural planes in boreholes of any azimuth was presented [32]. This method converts the coordinates of three arbitrary points in the 2D unfolded views into spatial coordinates to calculate the attitudes of the structural planes. However, this method suffers low calculation precision due to the few and untypical selected points. This will be discussed in detail in the following section.

To meet the two major challenges in the borehole TV imaging technology when applied in horizontal directional drilling, this study proposes an optimization algorithm for extracting the attitudes of structural planes based on borehole TV images in order to expand the application scope and improve the calculation precision of the technology. Moreover, this study develops a cable-free, storage-based TV device for boreholes of any azimuth. The effective combination of the optimization algorithm and the borehole TV device forms a new borehole TV imaging technology suitable for horizontal directional drilling. This new technology was used to test the attitudes of complete and incomplete structural planes. The test results show that the new technology proposed in this study can yield the attitudes of structural planes with required accuracy and can effectively meet the production requirements.

2. Borehole TV-Based Algorithm for Structural Plane Attitudes

2.1. Mathematical Model. The structural planes of rock masses are not always regular. Quite complex structural planes may be encountered in engineering practice. This study presents some structural planes in horizontal borehole 6# for the diversion project from the Dadu River to the Minjiang River. As shown in Figure 1(a), structural planes L1 and L2 do not intersect with other structural planes, so the 2D unfolded view exhibits regular sine curves. As shown in Figure 1(b), structural planes L3, L4, and L5 have missing parts in the 2D unfolded view due to the drop of blocks (see the shadow part in the figure). Structural planes L6 and L7 are cut by the structural plane L8, leaving only a little information on the 2D unfolded view. The structural plane penetration cannot be effectively analyzed if the information is ignored completely. However, current algorithms fail to locate the highest and lowest points, which are difficult to determine in these situations.

Figure 2 shows the schematic of the mathematical model of an incomplete structural plane. According to this figure, the borehole azimuth has a dip direction of α_0 and a dip angle of β_0. A coordinate system was set according to the right-hand rule. It is a local coordinate system rather than a geodetic coordinate system. The 2D unfolded view took the highest edge of gravity as its coordinate origin, the rotation angle of the borehole TV probe as its horizontal axis, and the current depth of the borehole as its vertical axis. The structural plane is present as a sinusoidal curve in the 2D unfolded view. Points P1–P6 are selected points on the structural plane. The mathematical problem discussed in this study is to calculate the dip direction and dip angle of the structural plane in the geodetic coordinate system based on the multipoint coordinate information on the 2D unfolded view through coordinate transformation and vector calculation.

2.2. Algorithm Flow. The algorithm flow in this study is shown in Figure 3. First, the coordinates of key points are selected in the 2D unfolded view for sinusoidal function fitting. Three spatial points are generated if the fitting results are acceptable. Otherwise, the key points are reselected.

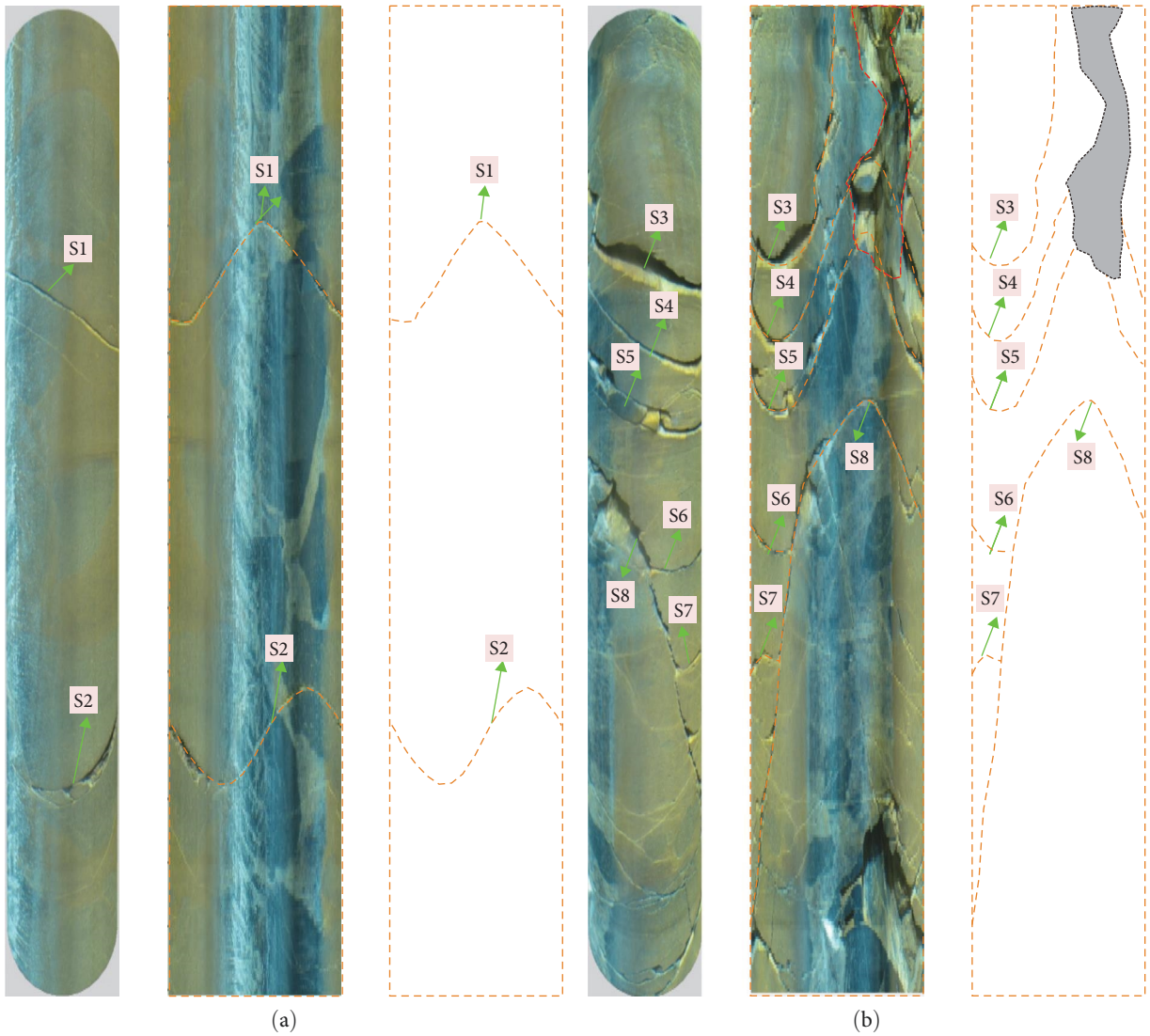

Figure 1: The structural planes of rock masses. (a) Complete structural planes. (b) Incomplete structural planes.

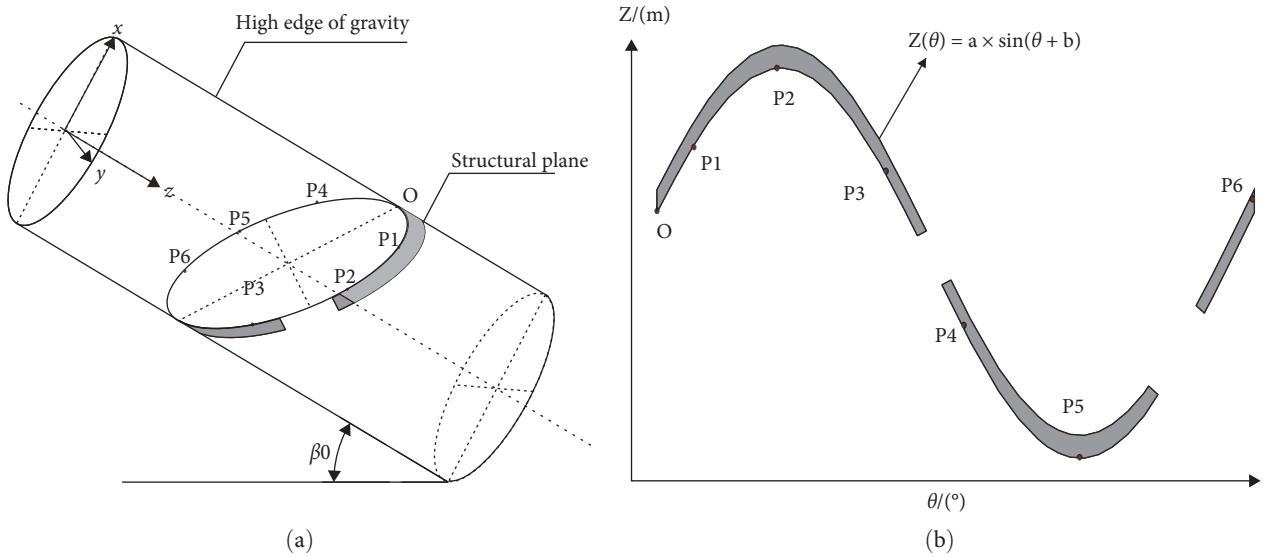

Figure 2: Mathematical model sketch. (a) Structural plane in a 3D digital core. (b) Structural plane in the 2D unfolded view.

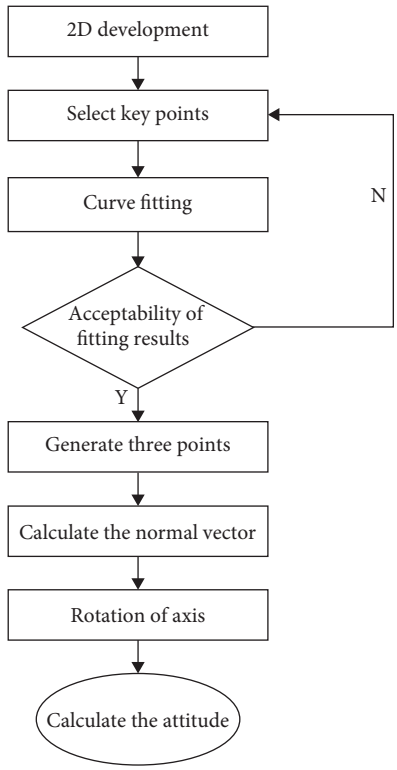

Figure 3: Algorithm flowchart.

Then, the normal vector is calculated using the coordinates of the generated space points. Subsequently, the coordinate axes are rotated. Finally, the attitude of the structural plane is calculated using the normal vector after rotation.

(1) Information of multiple points is used for sinusoidal curve fitting. The coordinates of the key points are set at:

$$\theta = [\theta_1, \theta_2, \ldots \theta_i, \ldots, \theta_n], \tag{1}$$

$$Z = [Z_1, Z_2, \ldots, Z_i, \ldots, Z_n], \tag{2}$$

where θ_i and Z_i are the horizontal and vertical coordinates of the ith point in the 2D unfolded view of the borehole.

The following function fitting is performed for the selected multipoint coordinates:

$$Z(\theta) = a \times \sin(\theta + b) + c, \tag{3}$$

where $Z(\theta)$ is the current borehole depth, and a, b, and c are fitting constants.

The fitting can be transformed into an extremum problem, that is, the undetermined coefficients a, b, and c are calculated to minimize the following equation:

$$S = \sum(a \times \sin(\theta_i + b) + c - Z_i)^2 \tag{4}$$

(2) Three arbitrary points are constructed based on the fitted function:

$$\begin{aligned} &A(R^*\cos(0), R^*\sin(0), Z(0)) \\ &B(R^*\cos(\theta_1'), R^*\sin(\theta_1'), Z(\theta_1')), \\ &C(R^*\cos(\theta_2'), R^*\sin(\theta_2'), Z(\theta_2')) \end{aligned} \tag{5}$$

where R is the borehole radius, and $\theta 1$' and $\theta 2$' are any nonzero and unequal angle values.

(3) The normal vector of the plane determined by points A, B, and C can be determined from the constructed spatial coordinates through the cross-product calculation between vectors:

$$\vec{N_0} = \vec{BA} \times \vec{CA}, \tag{6}$$

where $\vec{N_0}$ is the normal vector of plane ABC, $\vec{BA}$ is the vector from point B to point A, and $\vec{CA}$ is the vector from point C to point A.

(4) Transformation of coordinate axes: The normal vector calculated from Equation (7) is the dip direction and angle of the structural plane under the working face. To obtain the actual attitude of the structural plane, the coordinate system, as shown in Figure 1, must be rotated to the geodetic coordinate system. The dip direction and angle of the borehole are set at α_0 and β_0, respectively. First, the Y-axis is fixed and the coordinate system, as shown in Figure 1, is rotated by $(\pi/2 - \beta_0)$ around the Y-axis to make the Z-axis vertical. Then, the Z-axis is fixed and the coordinate system is rotated by $(\alpha_0 + 180)$ around the Z-axis to make the X-axis coincide with due north.

According to the equation for the rotation of the axes in the Cartesian coordinate system, rotating $\vec{N_0}$ by $(\pi/2 - \beta_0)$ around the Y-axis yields the normal vector $\vec{N_1}$ after rotation:

$$\vec{N_1} = \begin{bmatrix} \cos(R_y) & 0 & \sin(R_y) \\ 0 & 1 & 0 \\ -\sin(R_y) & 0 & \cos(R_y) \end{bmatrix} * \vec{N_0}', \tag{7}$$

where $R_y = \pi/2 - \beta_0$.

Rotating $\vec{N_1}$ by $(\alpha_0 + 180)$ around the Z-axis yields the normal vector after rotation $\vec{N_2}$:

$$\vec{N_2} = \begin{bmatrix} \cos R_z & -\sin R_z & 0 \\ \sin R_z & \cos R_z & 0 \\ 0 & 0 & 1 \end{bmatrix} * \vec{N_1}, \tag{8}$$

where $R_z = \alpha_0 + 180$.

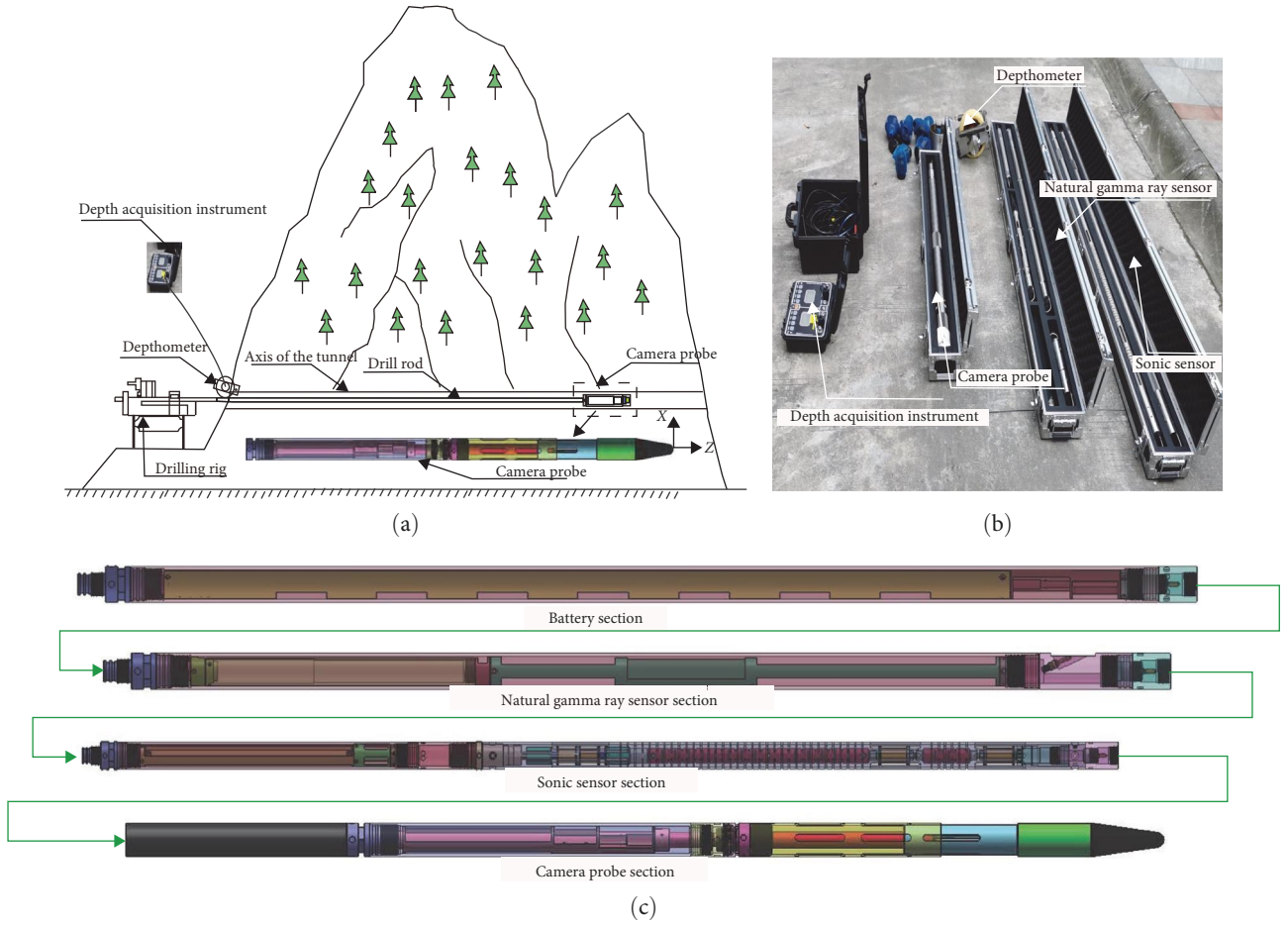

FIGURE 4: Borehole TV device. (a) Storage-based borehole TV for horizontal drilling. (b) Borehole TV device developed. (c) Camera probe section coupled with other geophysical sensors.

(5) The normal vector $\vec{N_2}$ is used to calculate the dip angle α of the structural plane, which is the dihedral angle between the structural plane and the horizontal plane. The normal vector of the horizontal plane is set at $D = [001]$. The dihedral angle is calculated as follows:

$$\alpha = \arccos\left(\left|\frac{D \times N_2}{|D| \times |N_2|}\right|\right). \tag{9}$$

According to the definition of the dip direction of the structural plane, the dip direction is always calculated using the upward normal vector. That is, the third component of the normal vector must be positive.

Setting $N_2 = [x_2, y_2, z_2](z_2 > 0)$, then:

$$e_0 = \arctan(abs(y_2/x_2)) \times 180/\pi, \tag{10}$$

where x_2, y_2, z_2 are the three coordinate components of the normal vector, respectively, and e_0 is the calculated value of the dip direction of the structural plane.

Considering different quadrants, the dip direction β should be calculated as follows:

$$\beta = \begin{cases} e_0 & (x_2 \geq 0, y_2 \geq 0) \\ 180 - e_0 & (x_2 \geq 0, y_2 \leq 0) \\ 180 + e_0 & (x_2 \leq 0, y_2 \leq 0) \\ 360 - e_0 & (x_2 \geq 0, y_2 \leq 0) \end{cases}, \tag{11}$$

where β is the dip direction of the structural plane, and x_2, y_2, z_2 are the three coordinate components of the normal vector, respectively.

3. Cable-Free, Storage-Based TV Device for Boreholes of Any Azimuth

Based on the optimization algorithm for structural planes proposed in this study, the authors of this study developed a cable-free, storage-based TV device for boreholes of any azimuth (see Figure 4(a)), which is directly connected to the drill rod through a connector and is directly pushed forward through a horizontal drilling rig. A depthometer is installed at the borehole opening, and the depth is obtained based on the friction between the drill rod and the depthometer. The cable-free and storage-based device can work normally in the temperature range of 0–125°C, and it can work normally for more than 8 hr.

Figure 5: Experiment photos. (a) Complete structural plane tested. (b) Simulated incomplete structural plane. (c) Pushing forward of camera probe.

Figure 4(b) shows an image of an actual borehole TV device developed in this study, which is mainly composed of a borehole TV probe, a depth acquisition instrument, a depthometer, and an intelligent borehole TV analysis system. Among them, the storage-based borehole TV probe includes a high-definition 2-megapixel camera, an electronic compass, and rechargeable batteries.

Compared with other existing devices, this device is cable-free and is characterized by low cost, low probability of damage caused by being stuck, and a deeper logging depth. Through flexible connection, this device can be easily combined with other geophysical methods, such as the acoustic, borehole temperature, and natural gamma-ray logging (see Figure 4(c)). A disadvantage of this device is that the acquired data cannot be transmitted to the borehole opening in real time but can only be read and analyzed after the probe is taken out. Moreover, since the depthometer is installed at the borehole opening, it is necessary to consider the precise synchronization between the depth, attitude data, and image data. This function is achieved using the self-developed depth acquisition instrument.

4. Process and Result Analysis of Laboratory Experiments

4.1. Laboratory Experiment Process. Laboratory experiments were conducted using the aforementioned borehole TV imaging device, and the main steps are as follows:

(1) The electronic compass in the borehole TV probe was calibrated. As a result, the sensor azimuth had an error of less than 1.5°.

(2) A laser azimuth instrument was developed to test the attitudes of complete structural planes. This instrument can emit lasers and project them into ellipses on an acrylic tube to simulate the structural planes of rock masses. The laser azimuth instrument was connected to a computer via Bluetooth for the purpose of real-time reading the attitudes of structural planes (see Figure 5(a)).

(3) Incomplete structural planes were simulated by forming fractures through cutting on an aluminum tube with a length of 2.5 m and an inner diameter of 66 mm (see Figure 5(b)). The actual attitudes of incomplete structural planes were recorded using the compass.

(4) A push rod was connected to the borehole TV probe with an outer diameter of 60 mm. A centralizer was set around the probe, and a depthometer was installed (see Figure 5(c)). The borehole TV probe was pushed forward using the push rod, and the depthometer was used to achieve the temporal synchronization between depth and video, with millisecond precision.

(5) The video and depth files were imported into an intelligent borehole TV analysis system for structural plane analysis. Moreover, the deviation between the testing results and the true attitudes was compared.

4.2. Testing Results of Complete Structural Planes. The acrylic tube used in laboratory experiments had an inner diameter of 66 mm and a length of 3 m. Two self-developed laser

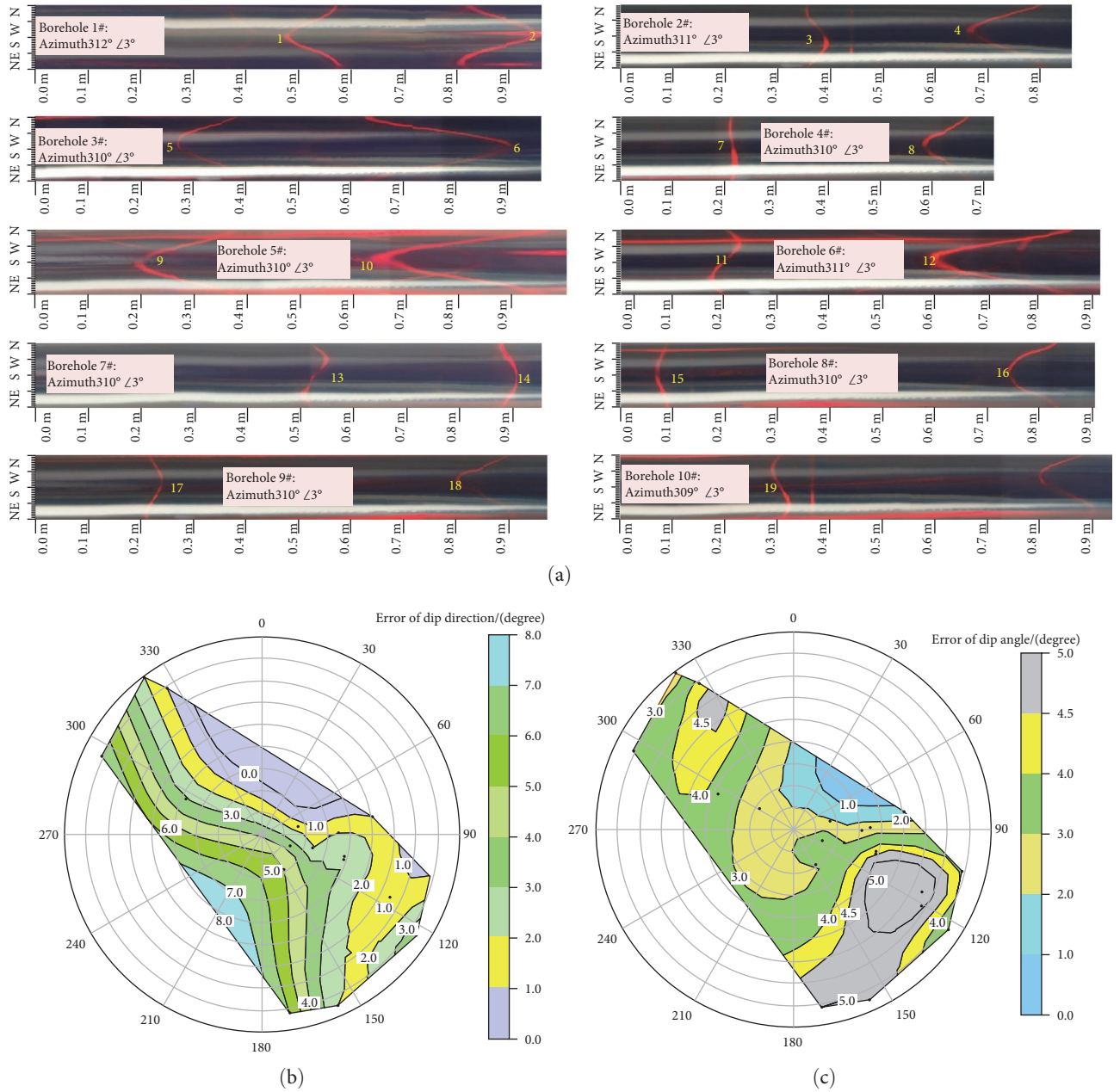

FIGURE 6: Testing results of complete structural planes. (a) Borehole TV images of complete structural planes. (b) Polar coordinate contour map of dip direction errors. (c) Polar coordinate contour map of dip angle errors.

azimuth instruments were employed for each experiment, during which information on two structural planes was obtained. Twenty complete structural planes were tested in the laboratory. The test samples included complete structural planes with steep and gentle dip angles in various quadrants.

Figure 6(a) shows the 2D unfolded views of the structural planes, which present clear images with high contrast. Some interference projections were generated due to the mutual interference of two laser azimuth instruments, but they did not affect the calculation of structural planes. As shown in Figures 6(b) and 6(c), the radial coordinate represents the dip angle, the tangential coordinate represents the dip direction, and the black spots represent the test samples. The test results show that the cable-free, storage-based TV device for boreholes of any azimuth yielded high-precision analytical results of complete structural planes, with dip direction errors of less than 10° and dip angle errors of less than 5°.

4.3. Testing Results of Incomplete Structural Planes. Discontinuous structural planes are widely present in actual logging processes. Therefore, it is necessary to verify the applicability of the algorithm proposed in this study to the calculation of incomplete structural planes. An aluminum tube with a length of 2.5 m and an inner diameter of 66 mm was employed in the laboratory experiment on discontinuous structural planes. Several nonpenetrating fractures were

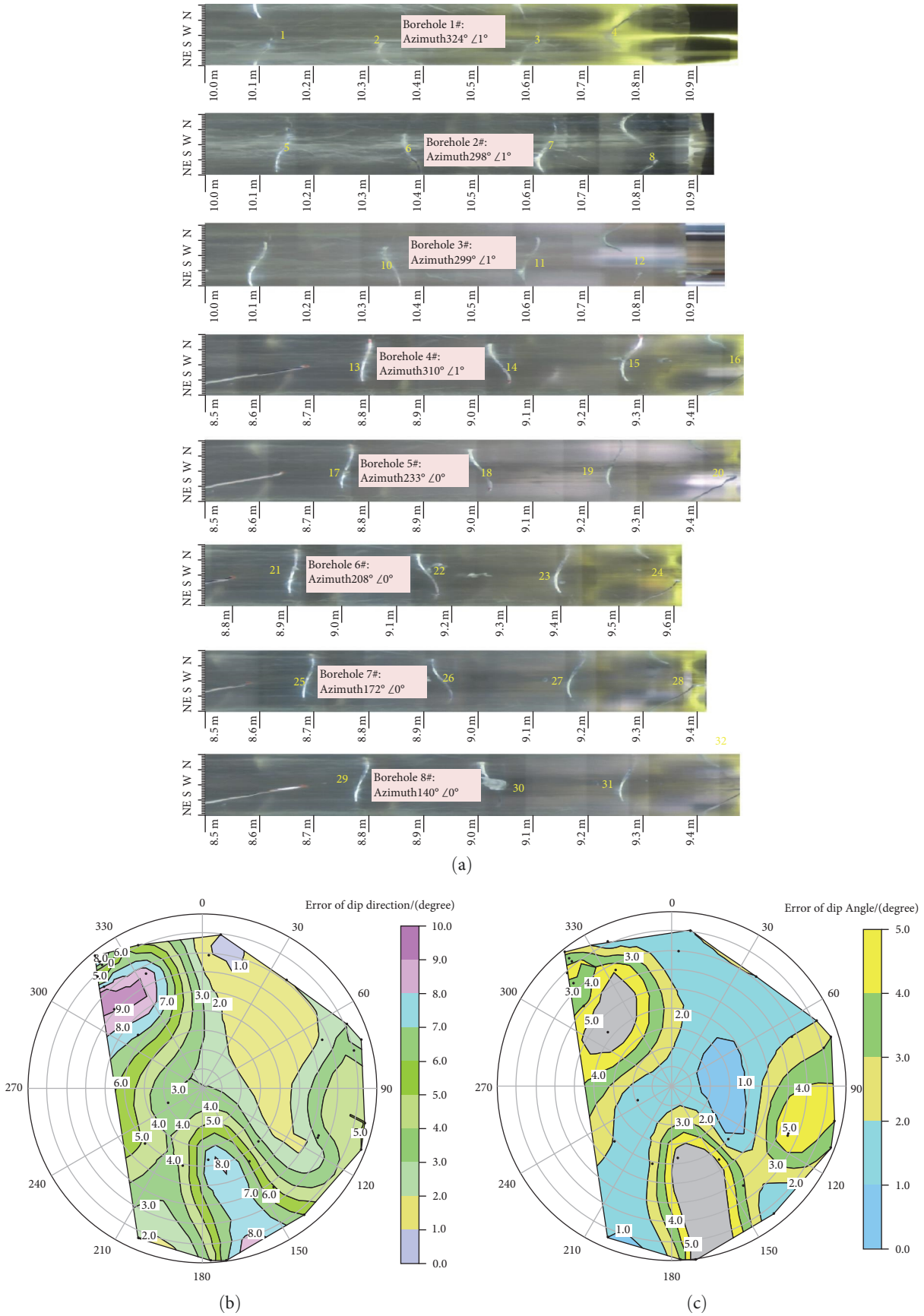

Figure 7: Testing results of incomplete structural planes. (a) Borehole TV images of incomplete structural planes. (b) Polar coordinate contour map of dip direction errors. (c) Polar coordinate contour map of dip angle errors.

Table 1: Results of the comparative analysis.

No.	Actual attitude	Algorithm of this study		Algorithm A		Algorithm B	
		Key points	Calculated attitude	Key points	Calculated attitude	Key points	Calculated attitude
1	289°∠27°	P1 (73.12°, 8.516 m) P2 (109.69°, 8.568 m) P3 (135.00°, 8.641 m) P4 (168.75°, 8.677 m)	280°∠28°	P1 (28.12°, 8.501 m) P2 (208.2°, 8.712 m)	289°∠37°	P1 (73.12°, 8.516 m) P2 (109.69°, 8.57 m) P3 (135.00°, 8.64 m)	313°∠68°
2	66°∠78°	P1 (92.81°, 8.800 m) P2 (240.47°, 8.816 m) P3 (282.66°, 8.822 m) P4 (317.81°, 8.824 m)	67°∠79°	P1 (120.94°, 8.798 m) P2 (300.94°, 8.819 m)	65°∠82°	P1 (92.81°, 8.800 m) P2 (240.47°, 8.816 m) P3 (282.66°, 8.822 m)	79°∠70°
3	206°∠89°	P1 (85.78°, 9.077 m) P2 (136.41°, 9.073 m) P3 (189.84°, 9.060 m) P4 (271.41°, 9.038 m)	206°∠84°	P1 (98.44°, 9.077 m) P2 (278.44°, 9.037 m)	205°∠86°	P1 (85.78°, 9.077 m) P2 (136.41°, 9.073 m) P3 (189.84°, 9.060 m)	208°∠89°
4	227°∠45°	P1 (0.00°, 9.416 m) P2 (87.19°, 9.450 m) P3 (181.41°, 9.492 m) P4 (326.25°, 9.403 m)	221°∠44°	P1 (344.53°, 9.407 m) P2 (164.53°, 9.492 m)	216°∠45°	P1 (0.00°, 9.416 m) P2 (87.19°, 9.450 m) P3 (181.41°, 9.492 m)	237°∠41°

formed on the tube through cutting to simulate incomplete rock structural planes. The attitudes of 32 structural planes were tested by changing the dip direction, dip angle, and rotation angle of the aluminum tube in the experiment (see Figure 7). The test samples included relatively complete and incomplete structural planes with steep, gentle, and moderate dip angles. As shown in Figures 7(b) and 7(c), the cable-free, storage-based TV device for boreholes of any azimuth yielded high-precision analytical results of the structural planes, with dip direction errors of less than 10° and dip angle errors of less than 5°. Therefore, this device applies to various structural planes, including relatively complete and incomplete structural planes with steep and gentle dip angles, thus meeting the production requirements.

4.4. Comparative Analysis. To further illustrate the superiority of the optimization algorithm proposed in this study, the optimization algorithm was compared with existing algorithms A and B. The results of the comparative analysis are shown in Table 1, which lists the actual attitudes of structural planes, the coordinates of key points involved in the algorithms, and the calculation results of the algorithms.

In algorithm A, the highest and lowest points in the 2D unfolded view were selected to calculate the attitudes of structural planes under the coordinates of the working face. This study supplemented algorithm A with coordinate axis transformation [31]. In algorithm B [32], three arbitrary points in the unfolded view were selected to construct the spatial coordinate system, and then the normal vector of the plane determined by the three points was calculated, followed by the rotation of the spatial coordinate system. As indicated by the results, (1) algorithm A failed to accurately locate the highest and lowest points of incomplete structural planes (e.g., structural plane No. 1), suffering high calculation errors, and this algorithm exhibited high calculation precision for relatively complete structural planes; (2) the calculation results of algorithm B largely depended on the selected points, with high calculation errors of the attitude. Compared with algorithms A and B, the optimization algorithm proposed in this study can utilize information on multiple points in the 2D unfolded view and allows manual adjustment of the selected points. As a result, the fitted curve is closer to the original structural plane, and thus the optimization algorithm has higher calculation precision. In addition, it is unnecessary to select the highest and lowest points of a structural plane in the optimization algorithm, which, therefore, is applicable to incomplete structural planes.

5. Conclusions

This study proposed an optimization algorithm for extracting structural plane characteristics based on borehole TV imaging. Using this algorithm, the attitudes of structural planes can be obtained through curve fitting using information on multiple points in the 2D unfolded view followed by spatial coordinate transformation. The optimization algorithm is highly practical for incomplete structural planes and structural planes with steep and gent dip angles.

Based on the optimization algorithm for structural planes, this study successfully developed a cable-free, storage-based TV device for boreholes of any azimuth. The optimization algorithm is feasible as verified through the laboratory experiments on 20 complete structural planes and 32 incomplete structural planes. The attitudes of structural planes measured using the device developed in this study have dip direction errors of less than 10° and dip angle errors of less than 5°. Therefore, the device can meet the production requirements.

Data Availability

The authors confirm that the data supporting the findings of this study are available within the article and its supplementary materials.

Conflicts of Interest

The authors declare that they have no known competing financial interests or personal relationships that may influence this study.

Acknowledgments

This study was supported by a Geological Survey Project of China (grant number: DD20230451) and the National Key R&D Program of China (grant number: 2019YFC1509904).

Supplementary Materials

Table S1: testing results of complete structural planes (unit: °). Table S2: test results of incomplete structural planes (unit: °). (*Supplementary Materials*)

References

[1] X. Zhengxuan, L. Jianguo, W. Jinsheng et al., "Application of ultra-deep directional drilling technology in the investigation of Sichuan–Tibet railway tunnel xu," *Advanced Engineering Sciences*, vol. 54, no. 2, pp. 22–29, 2022.

[2] J. S. Wu, X. L. Luo, X. Xu et al., "Construction overview and key technology for the horizontal directional coring test hole on plateau railway," *Drilling Engineering*, vol. 49, no. 6, pp. 1–7, 2022.

[3] J. Wan, S. Jiang, Y. Xia, J. Li, and G. Li, "Numerical model and program development of horizontal directional drilling for non-excavation technology," *Environmental Earth Sciences*, vol. 80, no. 17, pp. 1–21, 2021.

[4] J. Li, Y. Li, X. G. Xie et al., "Research and application of the logging evaluation method for horizontal holes in the main channel of Shiziyang," *Drilling Engineering*, vol. 49, no. 6, pp. 21–29, 2022.

[5] B. Ma, Y. Cheng, J. Liu, D. Zhu, X. Yan, and Q. Zhao, "Tunnel accurate geological investigation using long-distance horizontal directional drilling technology," *Tunnel Construction*, vol. 41, no. 6, pp. 972–978, 2021.

[6] S. C. Li, H. P. Wang, Q. H. Qian et al., "In-situ monitoring research on zonal disintegration of surrounding rock mass in deep mine roadways," *Chinese Journal of Rock Mechanics and Engineering*, vol. 27, no. 8, pp. 1546–1553, 2008.

[7] S. E. Prensky, "Advances in borehole imaging technology and application," in *Borehole Imaging: Applications and Case*

Histories, M. Lovell, G. Williamson, and P. K. Harvey, Eds., pp. 1–43, Geological Society, London, 1999.

[8] M. Eiichirou, O. Takashi, and I. Hiromistu, "Stratal border identification by image processing using a borehole tv system," *IEEJ Transactions on Electronics, Information and Systems*, vol. 10, no. 118, pp. 1522–1528, 1998.

[9] M. MŁynarczuk, "Description and classification of rock surfaces by means of laser profilometry and mathematical morphology," *International Journal of Rock Mechanics and Mining Sciences*, vol. 47, no. 1, pp. 138–149, 2010.

[10] N. Skoczylas and K. Godyń, "Evaluating selected lithological features using photographs taken with an introscopic camera in boreholes," *International Journal of Rock Mechanics and Mining Sciences*, vol. 72, pp. 319–324, 2014.

[11] M. Młynarczuk, M. Habrat, and N. Skoczylas, "The application of the automatic search for visually similar geological layers in a borehole in introscopic camera recordings," *Measurement*, vol. 85, pp. 142–151, 2016.

[12] S. I. Özkaya, "KINKFOLD—an AutoLISP program for construction of geological cross-sections using borehole image data," *Computers & Geosciences*, vol. 28, no. 3, pp. 409–420, 2002.

[13] T. Malone, B. Hubbard, D. Merton-Lyn, P. Worthington, and R. Zwiggelaar, "Borehole and ice feature annotation tool (BIFAT): a program or the automatic and manual annotation of glacier borehole images," *Computers & Geosciences*, vol. 51, pp. 381–389, 2013.

[14] X. J. Tan, J. Q. Zhang, F. W. Liu, X. M. Fu, and B. B. Kuang, "R&D of high-resolution digital borehole TV technology and its application in hydropower project," *Journal of Yangtze River Scientific Research Institute*, vol. 29, no. 8, pp. 62–66, 2012.

[15] L. Cheng, Q. Z. Wu, K. K. Hou, X. Q. Liu, Y. Liu, and B. B. Kuang, "Determination of the height of water-conducting fissure zone based on borehole TV imaging," *Gold*, vol. 42, no. 3, pp. 44–47, 2021.

[16] X. Wei and C. H. Yang, "A method of geometric parameter determination of drilling rock fractures," *Chinese Journal of Rock Mechanics and Engineering*, vol. 34, no. 9, pp. 1759–1765, 2015.

[17] Q. Guo, X. R. Ge, and A. L. Che, "Analysis on discontinuities connection basing on borehole photography method," *Journal of Shanghai Jiaotong University*, vol. 45, no. 5, pp. 734–737, 2011.

[18] W. W. Xu, B. Winkelman, T. Wilkinson et al., "Predict sandstone distribution by integrated study of deformed shale using borehole image and seismic data, a case study from northern Gulf of Mexico," *Petroleum Research*, vol. 5, no. 2, pp. 103–111, 2020.

[19] Q. Li, C. Zhang, Y. Yang U. Ansari, Y. Han, X. Li, and Y. Cheng, "Preliminary experimental investigation on long-term fracture conductivity for evaluating the feasibility and efficiency of fracturing operation in offshore hydrate-bearing sediments," *Ocean Engineering*, vol. 281, p. 114949.

[20] Q. Li, D. Zhao, J. Yin et al., "Sediment instability caused by gas production from hydrate-bearing sediment in Northern South China Sea by horizontal wellbore: evolution and mechanism," *Natural Resources Research*, vol. 32, no. 4, pp. 1595–1620, 2023.

[21] F. Wang, X. Liu, B. Jiang et al., "Low-loading Pt nanoparticles combined with the atomically dispersed FeN4 sites supported by FeSA-N-C for improved activity and stability towards oxygen reduction reaction/hydrogen evolution reaction in acid and alkaline media," *Journal of Colloid and Interface Science*, vol. 635, pp. 514–523, 2023.

[22] L. Li, B. Huang, Y. Tan, X. Deng, Y. Li, and H. Zheng, "Geometric heterogeneity of continental shale in the Yanchang Formation, Southern Ordos Basin China," *Scientific Reports*, vol. 7, no. 1, pp. 1–12, 2017.

[23] C. Wang, Y. Wang, Z. Han, J. Wang, and X. Zou, "A system for measuring borehole diametric deformation based on mechanical contact and micro-optical imaging," *Measurement*, vol. 130, pp. 191–197, 2018.

[24] K. Miyakawa, K. Tanaka, Y. Hirata, and M. Kanauchi, "Detection of hydraulic pathways in fractured rock masses and estimation of conductivity by a newly developed TV equipped flowmeter," *Engineering Geology*, vol. 56, no. 1-2, pp. 19–27, 2000.

[25] J. Hall, M. Ponzi, M. Gonfalini, and G. Maletti, "Automatic extraction and characterisation of geological features and textures from borehole images and core photographs," in *Proc. Soc. Petrophysicists Well-Log Analysts 37th Annu. Logging Symp.*, pp. 1–13, New Orleans, LA, USA, 1996.

[26] C. Wang, X. Zou, Z. Han, Y. Wang, and J. Wang, "An automatic recognition and parameter extraction method for structural planes in borehole image," *Journal of Applied Geophysics*, vol. 135, pp. 135–143, 2016.

[27] S. Yang, H. Li, L. Ma, and W. Bai, "An automatic method for discontinuity recognition in coal-measure strata borehole images," *IEEE Access*, vol. 9, pp. 105072–105081, 2021.

[28] C. Wang, X. Zou, Z. Han, J. Wang, and Y. Wang, "The automatic interpretation of structural plane parameters in borehole camera images from drilling engineering," *Journal of Petroleum Science and Engineering*, vol. 154, pp. 417–424, 2017.

[29] B. B. Thapa, P. Hughett, and K. Karasaki, "Semi-automatic analysis of rock fracture orientations from borehole wall images," *Geophysics*, vol. 62, no. 1, pp. 129–137, 1997.

[30] K. Glossop, P. J. G. Lisboa, P. C. Russell, A. Siddans, and G. R. Jones, "An implementation of the hough transformation for the identification and labelling of fixed period sinusoidal curves," *Computer Vision and Image Understanding*, vol. 74, no. 1, pp. 96–100, 1999.

[31] X. Zou, C. Wang, Y. Wang, and H. Song, "Morphological feature description method of structural surface in borehole image during in-situ instrumentation," *Rock Mechanics and Rock Engineering*, vol. 53, no. 7, pp. 2947–2956, 2020.

[32] D. Huang and Z. Zhong, "A universal mathematical method for determining occurrence of underground rock discontinuity based on TV picture of wall of a single borehole," *Earthscience-Journal of China University of Geosciences*, vol. 40, no. 6, pp. 1102–1106, 2015.